วารสารวิจัย UTK ราชมงคลกรุงเทพ

Synthesis, characterization and antimicrobial activity of organometallic Ru(II) complex containing phenylthiourea ligand

Rachna Neang[1], Parichad Chuklin[1], Saowanit Saithong[1], Sauwalak Phongpaichit[2], Luksamee Vittaya[3], Nararak Leesakul[1*]

[1]Department of Chemistry and Center for Innovation in Chemistry, Faculty of Science, Prince of Songkla University, Hat Yai, Songkhla
[2]Natural Products Research Center and Department of Microbiology, Faculty of Science, Prince of Songkla University, Hat Yai, Songkhla 90110, Thailand
[3]Faculty of Science and Fisheries Technology, Rajamangala University of Technology Srivijaya, Sikao, Trang
* Corresponding author: Tel.: 0 7428 8421 , Fax.: 0 7455 8841
E-mail: nararak.le@psu.ac.th

Abstract

A novel organometallic ruthenium(II)-*p*-cymene complex, [Ru(η^6-*p*-cymene)$(ptu)_2$Cl]SH, where ptu= *N*-phenylthiourea, was synthesized. Its structure was characterized by single crystal x-ray diffraction, elemental analysis and spectroscopic techniques (^{1}H-NMR and FTIR). The geometrical structure of the complex was tetrahedral, distorted by η^6 π-bonding to the p-cymene ring, with one chloro ligand and two molecules of ptu ligand. Antibacterial and antifungal activities were investigated. The [Ru(η^6-*p*-cymene)$(ptu)_2$Cl]SH complex produced MIC/MBC values of 32/32 µg/mL against methicillin resistant *Staphylococcus aureus* (MRSA), *Staphylococcus aureus* ATCC25923 (SA) and flucytosine-resistant *Cryptococcus neoformans* ATCC90113 flucytosine – resistant, CN90113 but apparently exhibited no antifungal against *Microsporum gypseum* clinical isolate.

Keywords: Ruthenium(II), Thiourea derivative, Antimicrobial activity

1. INTRODUCTION

The pathogenic bacteria *Staphylococcus aureus* (SA), Methicillin-resistant *Staphylococcus aureus* (MRSA) and *Escherichia coli* (EC) have a great impact on human health. Microorganisms with extensive resistance to antimicrobial agents cause serious health concerns in the global fight against infectious diseases [1-3].

Increasingly, more effective, less toxic treatments with wider ranges of activity are being developed from research in pharmaceutical inorganic chemistry, which is a branch of coordination chemistry [4, 5]. Considered to be versatile compounds, organometallic ruthenium (II) complexes have been extensively studied. Ru(II) can be coordinated through a strong bond with thiol groups [6] and can also form stable complexes with several types of monodentate nitrogen (N), oxygen (O) sulfur (S), and phosphine (P) donor ligands as well as with bidentate (S,O-; O,O-; N,O-; N,N-) ligands [7-9]. Ru (II) complexes acquire redox potential and permit electron transfer and ligand-ligand exchange due to the various +2, +3 and +4 oxidation states of the complexes [10, 11]. Its inertness towards displacement in arene substitution makes the ruthenium (II) ion stable in the

Received 06-06-2019
Revised 19-07-2019
Accepted 22-07-2019

+2 oxidation state [7]. Geometrically diverse Ru (II) complexes with a hydrophobic arene ligand and a hydrophilic metal center [12] can be stable in air [13, 14]. The Ru(II) complexes, $[Ru(\eta^6\text{-}p\text{-cymene})X_2]_2$ (X=Cl, I or NCS) and $[H_4Ru_4(\eta^6\text{-}p\text{-benzene})_4]^{2+}$ [13] have been reported biologically active.

Phenylthiourea is a derivative of thiourea. Its biological activities and applications were reported to be antiviral, antibacterial, antimalarial, antimicrobial, antitumor [15-17], and antifungal [18, 19]. Phenylthiourea and Ru(II) complexes are interesting compounds that present advantageous biotic activity. They are emerging in the pharmaceutical and medical fields through a variety of evolving processes.

Here we report an organometallic ruthenium compound with a half-sandwich, tetrahedral geometry distorted by η^6 π-bonding to the phenyl ring on Ru(II). The compound comprises one chloro ligand and two molecules of ptu ligand. The complex is evolving as a promising antibacterial and antifungal agent.

2. MATERIALS AND METHODS

Material

All chemicals purchased for this study were used as received. $[RuCl(\eta^6\text{-p-cymene})(\mu\text{-Cl})]_2$ was obtained from Merck. Chloroform, dichloromethane, acetonitrile and diethyl ether solvents were reagent grade purchased from RCI Labscan.

2.1 Instrumentation

The melting point of the obtained complex was determined using Thomas-Hoover, Unimelt 0-360 ^oC equipment. Elemental analysis data was acquired by CHNS-O Analyzer, (CEvInstruments Flash EA 1112 Series, Thermo Quest, Italy). FTIR spectra were produced between 4000 – 400 cm^{-1} on a BX Perkin Elmer FTIR spectrophotometer. Measurements were performed on samples pressed into KBr pellets. ^{1}H-NMR data were acquired on Varian BRUKER AVANCE 300 FT-NMR equipment and 300 MHz spectrometer using MeOH-d solvent. Tetramethylsilane ($Si(CH_3)_4$) was used as the internal standard. The absorption of the complex was recorded in the range of 200 – 400 nm on the Specord S100 model using a standard cuvette with a path length of 1 cm. Deuterium and tungsten were used as light sources for ultraviolet and visible regions, respectively.

A single crystal of [Ru(*p*-cymene)$(ptu)_2$Cl]SH was analyzed with a Bruker APEX-II CCD diffractometer using graphite-monochromated Mo Kα radiation (λ= 0.71073 Å). The diffraction pattern was formed from 33925 reflections. The raw data were interpreted by SMART, SAINT v8.34A and SADABS software [20] and the structure was solved by SHELXS [21]. All non-hydrogen was refined by the anisotropic thermal parameters. A riding model was used to refine calculations with all hydrogen atoms placed in ideal positions. The materials and molecular graphics for publication were prepared with the WinGXv2014.1 [22] and Mercury3.6 [23] programs. Crystallographic data of [Ru(*p*-cymene)$(ptu)_2$Cl]SH were placed in the Cambridge Crystallographic Data Center and can be provided on request, using the access code CCDC1917489, via http://www.ccdc.cam.ac.uk/data_request/cif (or from the Cambridge Crystallographic Data Centre, 12 Union Road, Cambridge CB21EZ, U.K.; fax: +44 1223 336 033 or email deposit@ccdc.cam.ac.uk). The X-ray data are presented in the supplementary data.

2.2 Synthesis pathway of [Ru(*p*-cymene) $(ptu)_2$Cl]SH complex

The novel complex of [Ru(*p*-cymene)$(ptu)_2$Cl]SH was synthesized by the reaction between *N*-phenylthiourea (ptu) with dichloro (p-cymene) ruthenium (II) dimer in a typical one-pot process, using

a solution of dichloro (p-cymene) ruthenium(II) dimer (0.306 g, 0.5 mmol) and *N*-phenylthiourea (ptu) (0.182 g, 1.0 mmol) in 20 ml of dichloromethane. The solution was left to evaporate at room temperature to reduce the mixture volume and was crystallized by adding 3 ml of acetonitrile. The obtained dark orange crystal was filtered and washed three times with chloroform (3 ml x 3). Yield: 43.45%. Melting point: 168 – 170 ºC. Anal Calcd. For RuC24H35N4S3ClO2 (644.59): C, 45.75; H, 5.48; N, 8.69. Found: C, 45.85; H, 4.78; N, 8.83. IR: 2970 (νsp^2 C-H), 1529 (νC=C), 1328 (νC_{ph}-N), 3219 (νN-H), 698 (νC=S), 891 (νC-H bending of para disubstituted benzene), 510 (δRu-S) cm^{-1}. ^{1}H NMR (300 MHz, CD_3OH) 8 signals: δ (ppm): 7.47 (t, 2H, JHH = 7.5 Hz), 7.35 (t, 4H, JHH = 7.5 Hz), 7.26 (d, 4H, JHH = 7.5 Hz), 5.64 (d, 2H, JHH = 5.5 Hz), 5.52 (d, 2H, JHH = 5.5 Hz), 2.93 (m, 1H, JHH = 7.0 Hz), 2.23 (s, 3H), 1.33 (d, 6H, JHH = 7.0 Hz).

2.3 Antimicrobial assay

The synthesized [Ru (*p*-cymene) $(ptu)_2$Cl]SH compound was tested against methicillin-resistant *Staphylococcus aureus* (MRSA) SK1, *Staphylococcus aureus* ATCC25923, and *Escherichia coli* ATCC25922 using a colorimetric modification method of the Clinical and laboratory standards institute (CLSI) M07-A9 [24], slightly modified. The testing compound was prepared in dimethyl sulfoxide (DMSO). Minimal inhibitory concentration (MIC) represents the lowest concentration of synthesized compound with violet color of resazurin indicating growth inhibition. The test media at MIC concentration and higher were dropped on nutrient agar plate and incubated under appropriate conditions. Minimal bactericidal concentration (MBC) was verified as no growth at the lowest concentration of the test compound. Vancomycin and gentamicin were used as the positive controls of antibacterial inhibition.

2.4 Antifungal assay

The MIC of the synthesized compound was tested against yeast (*Cryptococcus neoformans* ATCC90113), using a modification of the microbroth dilution CLSI M27-A3 [25] and against a clinical isolate of *Microsporum gypseum* MU-SH4, using a modification of the microbroth dilution CLSI M38-A2 [26]. The plates were incubated for 48 h at 35 ºC for *C. neoformans* and at room temperature for *M. gypseum* (MG). The streaking method on Sabouraud's dextrose agar was taken to determine the minimal fungicidal concentration (MFC) of the [Ru(*p*-cymene)$(ptu)_2$Cl]SH compound. A clinical standard of Amphotericin B was used as positive inhibitory control for yeast and miconazole for *M. gypseum* testing.

3. RESULTS AND DISCUSSION

Synthesis and characterization

The novel [Ru(*p*-cymene)$(ptu)_2$ Cl]SH complex was synthesized at ambient temperature by the reaction of Ru(II)-p-cymene with the N-phenylthiourea ligand through the S donor in dichloromethane (Scheme 1).

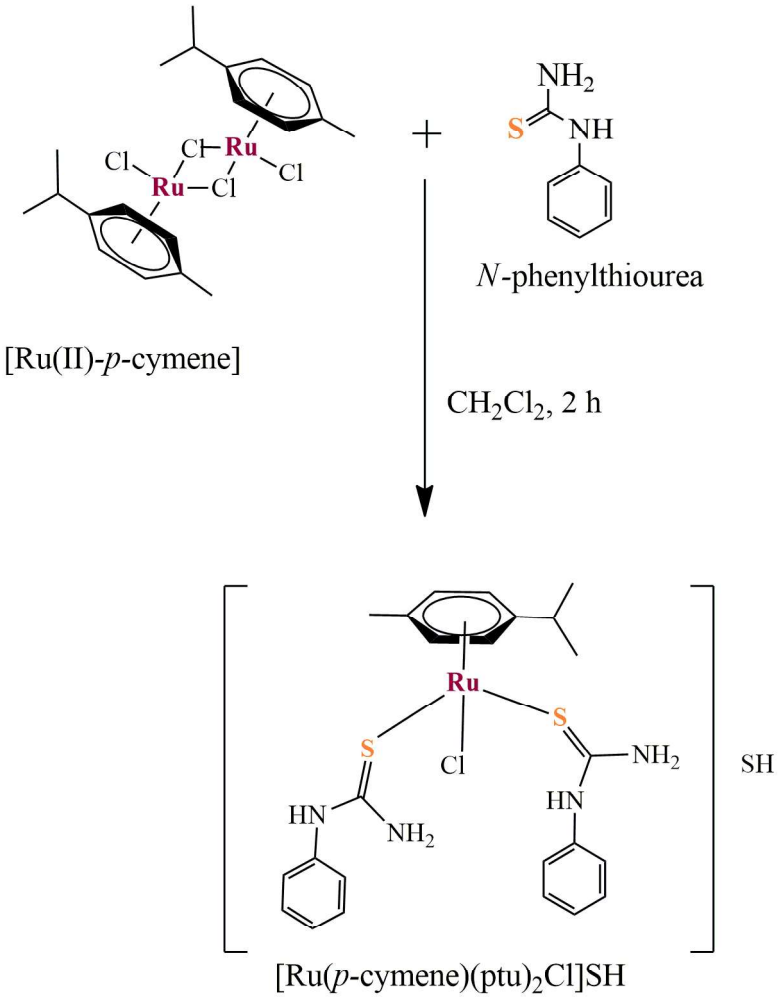

Scheme 1. Synthesis pathway of [Ru(*p*-***Figure*** cymene)$(ptu)_2$Cl]SH complex

To produce ^{1}H-NMR spectra, the [Ru(*p*-cymene)$(ptu)_2$Cl]SH complex was measured in solution in MeoH-d_6. The main characteristic peaks were identified for the phenyl ring on Ru(II) and the efficient ptu ligand. The coordination of Ru(II) with p-ptu ligands produced a downfield shift from 7.26 to 7.47 ppm. Similarly, the coordination with p-cymene ligands is located between 5.52 and 5.64 ppm (see from Index S1). Elemental analysis results confirmed the theoretical values for percentages of C, H and N atoms.

The FTIR characteristic spectrum of the [Ru(*p*-cymene)$(ptu)_2$Cl]SH complex (see from Index S2) displays peaks assigned to the ptu ligand coordinated to the Ru^{2+} metal center. As a result of this coordination, the shift in the vC=S vibrational frequency of the complex (698 cm^{-1}) occurred at a lower stretching frequency (789 cm^{-1}) than that of the free ptu ligand. As previously reported [27], this shift is due to electron π back-bonding from the d orbital of Ru^{2+} to the π* orbital of the ptu ligand. Also, an important vibrational frequency attributed to Ru-S stretching was detected at 510 cm^{-1}.

With regard to the obtained dark orange crystal, the crystallographic data of the [Ru(*p*-cymene)(ptu)$_2$Cl]SH complex is collected in Table 1 and Index S3. The Ru(II) complex exhibits a tetrahedral geometry distorted by η^6 π-bonding of the *p*-cymene ring, with one Cl atom and two molecules of ptu contributed by the S donor atom (Figure 1). Certain selected bond distances and bond angles are shown in Table 2. The Ru-Cl distance for Ru-Cl1 is 2.4160(6) Å, which approximately corresponds to distances reported for related complexes: [(η^6-*p*-cymene)RuCl$_2$ (PPh$_2$Py)], 2.4107 to 2.4111 Å [28] and [(η^6-*p*-cymene)Ru(3-acetylpyridine)Cl$_2$], 2.3986 to 2.1970 Å [29]. The interatomic distances Ru-S1 and Ru-S2 are 2.4106(6) and 2.3962(7) Å, respectively, which are close to distances reported for the complexes [(η^6-*p*-cymene) RuCl$_2$ (PPh$_3$) (imidazolidine-2-thione)] PF$_3$, 2.399(13) Å [31] and [(η^6-*p*-cymene)Ru(SCH$_2$COO]$_2$, 2.3943(11) to 2.3992(10) Å [31]. The distances for Ru-(p-cymene) are 2.159(2) to 2.253(2) Å, which are comparable to the distances reported for [(η^6-*p*-cymene)Ru(3-acetylpyridine)Cl$_2$], 2.154 to 2.1209 Å [29]. The angles S1-Ru1-Cl1 and S2-Ru1-Cl1 measure 90.42(3)^o and 87.63(2)^o, respectively, which correspond to measurements for the same angles in a related Ru(II) complex: 90.11(4)^o in [(η^6-*p*-cymene)RuCl$_2$(PPh$_3$) (imidazolidine-2-thione)]PF$_3$ [30]. The S1-Ru-S2 angle measures 80.19(2)^o, which is close to the angle of 80.71(4)^o in the related Ru(II) complex [(η^6-*p*-cymene)Ru(SCH$_2$COO]$_2$ [30]. The S atom of HS$^-$ (S3') interacts intermolecularly via H-bonding with the H1A, H2, and H3A atoms of the [Ru(*p*-cymene)(ptu)$_2$Cl]$^-$. The distances H1A…S3', H2…S3' and H3A…S3' are 3.374(2), 3.175(2) and 3.240(2) Å, respectively. In addition, the Cl atom interacts intramolecularly with the H1B atom via H-bonding with a distance of 3.231(2) Å (Figure 2, Figure 3 and Table 3).

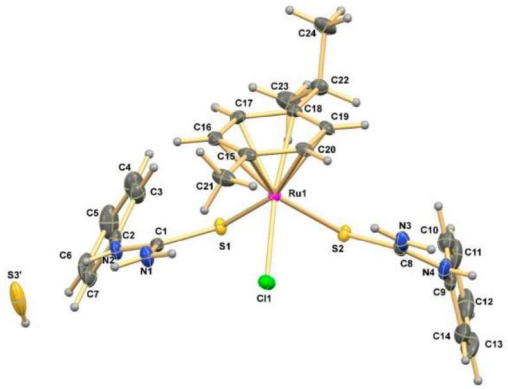

Figure 1. An ORTEP structure of the [Ru(*p*-cymene)(ptu)$_2$Cl]SH complex with numbered atoms

Table 1. Crystallographic data of the [Ru (*p*-cymene)(ptu)$_2$Cl]SH comple

Empirical formula	C24H31ClN4RuS3
Formula weight	608.23
Wavelength	0.71073 Å
Crystal system	Triclinic
Space group	$P\bar{1}$
Unit cell dimensions	*a*= 6.6265 Å
	b= 12.6582(4) Å
	c= 17.6833(4) Å
	α= 73.3800 (10)^o
	β= 80.8120 (10)^o
	γ= 75.5900 (10)^o
Temperature	273 (2) K
Z	2
Density (calculated)	1.474 Mg/m^3
Absorption coefficient	0.918 mm^{-1}
Volume	1370.31(7) Å^3
Goodness-of-fit on F^2	1.023
Final *R* indices [I>2σ(I)]	*R*1= 0.0317,
	wR2= 0.0669
R indices (all data)	*R*1= 0.0478,
	wR2= 0.0719

Table 2. Selected bond lengths (Å) and angle (°) for the [Ru(*p*-cymene)(ptu)$_2$Cl]SH complex

Lengths			
Ru(1)-C(17)	2.159(2)	Ru(1)-C(15)	2.253(2)
Ru(1)-C(19)	2.187(2)	Ru(1)-S(2)	2.3962(7)
Ru(1)-C(18)	2.198(2)	Ru(1)-S(1)	2.4106(6)
Ru(1)-C(16)	2.203(2)	Ru(1)-Cl(1)	2.4160(6)
Ru(1)-C(20)	2.216(2)	S(3')-H(3')	0.85(4)
Angles			
C(17)-Ru(1)-S(2)	124.07(7)	C(18)-Ru(1)-S(2)	95.05(7)
C(19)-Ru(1)-S(2)	91.63(7)	C(16)-Ru(1)-S(2)	161.98(7)
C(18)-Ru(1)-S(2)	95.05(7)	C(20)-Ru(1)-S(2)	114.55(8)
C(16)-Ru(1)-S(2)	161.98(7)	C(15)-Ru(1)-S(2)	150.77(8)
C(20)-Ru(1)-S(2)	114.55(8)	C(17)-Ru(1)-S(1)	86.06(7)
C(15)-Ru(1)-S(2)	150.77(8)	C(19)-Ru(1)-S(1)	140.98(7)
C(17)-Ru(1)-S(1)	86.06(7)	C(18)-Ru(1)-S(1)	104.50(7)
C(19)-Ru(1)-S(1)	140.98(7)	C(16)-Ru(1)-S(1)	97.44(8)
C(20)-Ru(1)-S(1)	163.27(8)	C(16)-Ru(1)-Cl(1)	110.31(7)
C(15)-Ru(1)-S(1)	129.00(8)	C(20)-Ru(1)-Cl(1)	97.78(7)
S(2)-Ru(1)-S(1)	80.19(2)	C(15)-Ru(1)-Cl(1)	90.31(7)
C(17)-Ru(1)-Cl(1)	146.74(7)	S(2)-Ru(1)-Cl(1)	87.63(2)
C(19)-Ru(1)-Cl(1)	127.58(7)	S(1)-Ru(1)-Cl(1)	90.42(2)

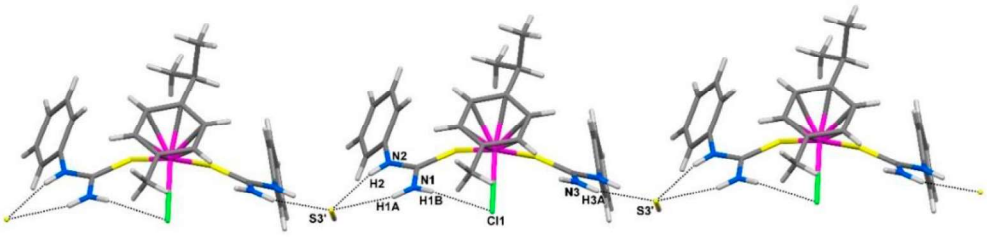

Figure 2. Hydrogen-bond interaction of [Ru(*p*-cymene)(ptu)$_2$Cl]SH complex

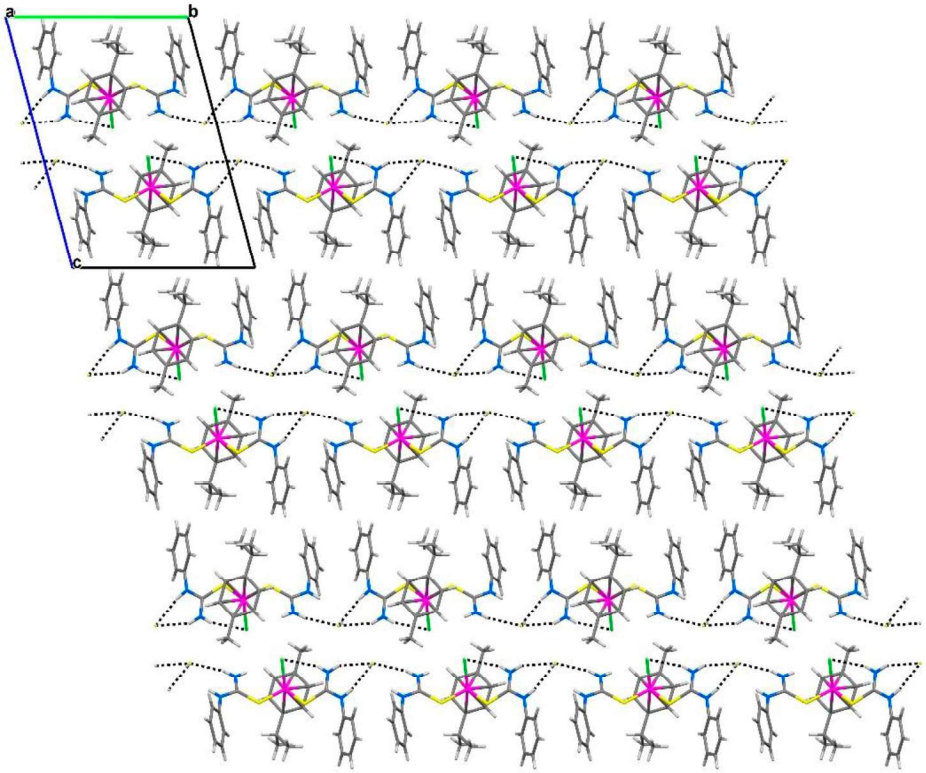

Figure 3. Hydrogen-bond packing interaction of [Ru(*p*-cymene)(ptu)$_2$Cl]SH

Table 3. Hydrogen-bond of [Ru(*p*-cymene)(ptu)$_2$Cl]SH complex

D-H…A	Distance of (D-H)	Distance of (H…A)	Distance of (D…A)	Angle of (DHA)
N(1)-H(1A)…S(3')	0.86	2.61	3.374(2)	148.9
N(1)-H(1B)…Cl(1)	0.86	2.50	3.231(2)	143.1
N(2)-H(2)…S(3')	0.86	2.33	3.175(2)	166.2
N(3)-H(3A)…S(3')#1	0.86	2.40	3.240(2)	166.2

D= N atom (donor), A= S or Cl atom (acceptor) Symmetry transformations used to generate equivalent atoms: #1 x-1, y+1, z

3.1 Antibacterial and antifungal assay

Antimicrobial activity was determined by colorimetric broth microdilution. The [Ru(*p*-cymene)(ptu)$_2$Cl]SH complex showed equal inhibition against Gram-positive bacteria of *S. aureus* (SA) and Methicillin-resistant *S. aureus* (MRSA) with the MIC/MBC values of 32/32 µg/mL. The [Ru(*p*-cymene)(ptu)$_2$Cl]SH complex also exhibited an inhibitory activity against yeast (*C. neoformans*, MIC/MFC 32/32 µg/mL) but it did not exhibit the inhibitory activity against *Microsporum gypseum* MU-SH4 clinical isolate, while the starting materials of the dinuclear complex of Ru_2Cl_4(p-cymene)$_2$ and free ptu ligand did not show inhibitory activity.

However, the MIC/MBC values of the commercial antibacterial drug like vancomycin and the MIC/MFC values of the commercial antifungal drug Amphotericin B indicate stronger activity than the [Ru(*p*-cymene)(ptu)$_2$Cl]SH complex (Table 4). This might be due to the lipophilic character of the synthesized complex which should be able to penetrate the cell membrane lipid layer of the studied bacteria and yeast. The experimental data revealed that the [Ru(*p*-cymene)(ptu)$_2$Cl]SH compound showed moderate antibacterial and antifungal activities.

Table 4. MIC and MBC or MFC values

Code	Bacteria (µg/mL)						Yeast(µg/mL)		Filamentous fungus (µg/mL)	
	SA		MRSA		EC		CN90113		MG	
	MIC	MBC	MIC	MBC	MIC	MBC	MIC	MFC	MIC	MFC
[Ru(*p*-cymene)(ptu)$_2$ Cl]SH	32	32	32	32	NA	NA	32	32	NA	NA
Ru_2Cl_4(p-cymene)$_2$	-	-	-	-	-	-	-	-	-	-
ptu	-	-	-	-	-	-	-	-	-	-
Vancomycin	0.5	1	1	2	-	-	-	-	-	-
Gentamicin	-	-	-	-	0.5	-	-	-	-	-
Amphotericin B	-	-	-	-	-	-	0.25	0.5	-	-

SA= *Staphylococcus aureus* ATCC25923, MRSA= methicillin-resistant *Staphylococcus aureus*, EC=*Escherichia coli* ATCC25922, CN90113= *Cryptococcus neoformans* ATCC90113 flucytosine-resistant, MG = *Microsporum gypseum* clinical isolate, MIC= minimal inhibitory concentration (µg/mL), MBC= minimal bactericidal concentration (µg/mL), MFC= minimal fungicidal concentration (µg/mL), NA = non active

4. CONCLUSIONS

The half sandwich [Ru(*p*-cymene)(ptu)$_2$Cl]SH complex has a distorted pseudo-tetrahedral geometry coordinated via the S donor of the ptu ligand. The complex exhibited moderate antibacterial and antifungal activity against methicillin-resistant *S. aureus* (MRSA), *S. aureus* ATCC25923 and flucytosin-resistant *C. neoformans* ATCC90113 with the value of MIC/MBC or MFC of 32/32 µg/mL.

5. ACKNOWLEDGMENTS

We would like to express our heartfelt thanks to the Royal Scholarship under Her Royal Highness Princess Maha Chakri Sirindhorn Education Project and Graduate School, Prince of Songkla University for giving the opportunity and financial support to Ms.Rachna Neang to study her Master's Degree at the Department of Chemistry, Faculty of Science. We also acknowledge the Center for Innovation in Chemistry (PERCH-CIC), the Commission on Higher Education and the Ministry of Education and Faculty of

Science, PSU for financial support. We also would like to thank the Natural Products Research Center and Department of Microbiology, Faculty of Science for the facilities used for antimicrobial activity testing and the Faculty of Science and Fisheries Technology, Rajamangala University of Technology Srivijaya, Trang campus for partial financial support. Authors would like to thank Mr.Thomas Duncan Coyne for assistance with the English.

6. REFERENCES

[1] Enright MC, Robinson DA, Randle G, Feil EJ, Grundmann H, Spratt BG. The evolutionary history of methicillin-resistant Staphylococcus aureus (MRSA). PNAS USA 2002; 99(11):7687-92.

[2] Elizaquivel P, Aznar R. Comparison of four commercial DNA extraction kits for PCR detection of Listeria monocytogenes, Salmonella, Escherichia coli O157:H7, and Staphylococcus aureus in fresh, minimally processed vegetables. J Food Protect 2008; 71(10):2110-4.

[3] Kabbani AT, Hammud HH, Ghannoum AM. Preparation and antibacterial activity of copper and cobalt complexes of 4-chloro-3-nitrobenzoate with a nitrogen donor ligand. Chem Pharm Bull 2007; 55(3):446-50.

[4] Beckford F, Dourth D, Shaloski M, Didion J, Thessing J, Woods J, Crowell V, Gerasimchuk N, Gonzalez-Sarrías A, Seeram NP. Half-sandwich ruthenium–arene complexes with thiosemicarbazones: Synthesis and biological evaluation of [(η^6-p-cymene) Ru (piperonalthiosemicarbazones) Cl] Cl complexes. J Inorg Biochem 2011; 105(8):1019-29.

[5] Sun D, Zhang W, Yang E, Li N, Liu H, Wang W. Investigation of antibacterial activity and related mechanism of a ruthenium(II) polypyridyl complex. Inorg Chem Commun 2015; 56:17-21.

[6] Zhang P, Sadler PJ. Advances in the design of organometallic anticancer complexes. J Organomet Chem 2017; 839:5-14.

[7] Pastuszko A, Majchrzak K, Czyz M, Kupcewicz B, Budzisz E. The synthesis, lipophilicity and cytotoxic effects of new Ruthenium(II) arene complexes with chromone derivatives. J Inorg Biochem. 2016; 159:133-41.

[8] Chuklin P, Chalermpanaphan V, Nhukeaw T, Saithong S, Chainok K, Phongpaichit S, Ratanaphan A, Leesakul N. Synthesis, x-ray structure of organometallic Ruthenium (II) p-cymene complexes based on P- and N-donor ligands and their in vitro antibacterial and anticancer studies. J Organomet Chem 2017; 846:242-50.

[9] Pantić DN, Aranđelović S, Radulović S, Roller A, Arion VB, Grgurić-Šipka S. Synthesis, characterisation and cytotoxic activity of organoruthenium (II)-halido complexes with 1H-benzimidazole-2-carboxylic acid. J Organomet Chem 2016; 819:61-8.

[10] Allardyce CS, Dyson PJ. Ruthenium in medicine: current clinical uses and future prospects. Platin Met Rev 2001;45(2): 62-9.

[11] Chen J, Peng F, Zhang Y, Li B, She J, Jie X, Zou Z, Chen M, Chen L. Synthesis, characterization, cellular uptake and apoptosis-inducing properties of two highly cytotoxic cyclometalated ruthenium(II) beta-carboline complexes. Eur J Med Chem 2017; 140:104-17.

[12] Raj KR, Ramesh R, Małecki J. Synthesis and structure of arene Ruthenium (II) benzhydrazone complexes: antiproliferative activity, apoptosis induction and cell cycle analysis. J Organomet Chem 2018; 862:95-104.
[13] Allardyce CS, Dyson PJ, Ellis DJ, Salter PA, Scopelliti R. Synthesis and characterisation of some water soluble ruthenium (II)–arene complexes and an investigation of their antibiotic and antiviral properties. J Organomet Chem 2003; 668(1):35-42.
[14] Nikolić S, Opsenica DM, Filipović V, Dojčinović B, Aranđelović S, Radulović S. Strong in vitro cytotoxic potential of new ruthenium–cymene complexes. Organometallics. 2015; 34(14):3464-73.
[15] Mansour AM. Structural studies and biological activity evaluation of Pd(II), Pt(II) and Ru(II) complexes containing N-phenyl, N`-(3-triazolyl) thiourea. Appl Organomet Chem 2018; 32(1):3928.
[16] Saeed S, Rashid N, Jones PG, Ali M, Hussain R. Synthesis, characterization and biological evaluation of some thiourea derivatives bearing benzothiazole moiety as potential antimicrobial and anticancer agents. Eur J Med Chem 2010; 45(4):1323-31.
[17] Shakeel A, Altaf A. Thiourea derivatives in drug design and medicinal chemistry: A Short Rev 2016;10 p.
[18] Criado JJ, Rodríguez-Fernández E, García E, Hermosa MR, Monte E. Thiourea derivatives of α-aminoacids. Synthesis and characterization of Ni(II), Cu(II) and Pt(II) complexes with l-valinate derivatives antifungal activity. J Inorg Biochem 1998; 69(1):113-9.
[19] Del CR, Criado JJ, García E, Hermosa MR, Jiménez-Sánchez A, Manzano JL, Monte E, Rodríguez-Fernández E, Sanz F. Thiourea derivatives and their Nickel(II) and Platinum(II) complexes: Antifungal activity. J Inorg Biochem 2002; 89(1):74-82.
[20] Bruker, SMART, SAINT and SADABS, Bruker AXS Inc, Madison,Wisconsin, USA, 2013.
[21] Sheldrick GM. Crystal structure refinement with SHELXL. Acta Crystallogr C 2015; 71(Pt 1):3-8.
[22] Farrugia L. WinGX and ORTEP for windows: an update. J Appl Crystallogr 2012; 45(4):849-54.
[23] Clare F, Macrae IJB, James AC, Paul RE, Patrick M, Elna P, Lucia R, Robin T, Jacco van de S, Peter AW. Mercury CSD 2.0 – new features for the visualization and investigation of crystal structures. Appl Crystallogr 2008; 41: 466–70.
[24] Franklin RC llI, MD Matthew AW, MD, MBA, FIDSA Jeff A, PhD Michael ND, PharmD, FIDSA George ME, MD Mary JF, PhD, MPH Dwight JH, PhD David WH, MD Janet AH, MCLS, MT(ASCP) Jean BP, PhD, D(ABMM) Mair P, MD, FRCP, FRCPath Jana MS, MMSc Richard BT, Jr, PhD Maria MT, BS, MT(ASCP) John DT, MD Melvin PW, MD Barbara LZ, PhD. Methods for dilution antimicrobial susceptibility tests for bacteria that grow aerobically; approved standard—ninth edition CLSI 2012;32.
[25] Clinical and Laboratory Standards Institute. Reference method for broth dilution antifungal susceptibility testing of yeasts; approved standard-Third edition. 2008.

[26] Clinical and Laboratory Standards Institute. Reference method for broth dilution antifungal susceptibility testing of filamentous fungi; approved standard- Second edition. 2008.
[27] Akinchan NT, Drożdżewski PM, Battaglia LP. Crystal structure and spectroscopic characterization of bis(N-phenylthiourea). J Chem Crystallogr 2002; 32(3):91-7.
[28] Ralte L, Patrick JC, Rao KM. Study of reactivity of p-cymene ruthenium(II) dimer towards diphenyl-2-pyridylphosphine : Synthesis, characterization and molecular structures of [(η^6-p-cymene)$RuCl_2(PPh_2Py)$] and [(η^6-p-cymene)$RuCl(PPh_2Py)]BF_4$. J Chem Sci 2004; 116(1):21-7.
[29] Grgurić-Šipka S, Ivanović I, Rakić G, Todorović N, Gligorijević N, Radulović S, Arion VB, Keppler BK, Tešić ŽLj. Ruthenium(II)–arene complexes with functionalized pyridines: Synthesis, characterization and cytotoxic activity. Eur J Med Chem 2010; 45(3):1051-8.
[30] Hanif M, Nawaz MA, Babak MV, Iqbal J, Roller A, Keppler BK. RutheniumII(eta^6-arene) complexes of thiourea derivatives: synthesis, characterization and urease inhibition. Molecules. 2014;19(6):8080-92.
[31] Henderson W, Kilpin TD, Nicholson BK. (p-cymene) thioglycollato ruthenium (II) dimer; a complex with an ambi-basic S, O-donor ligand. Struct Chem 2007;19(2):199-202.

Index

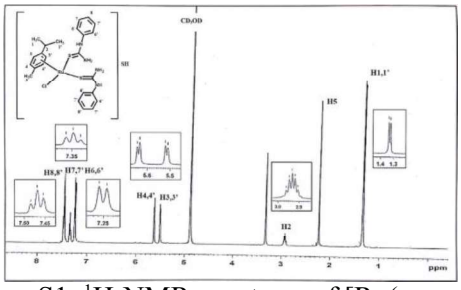

S1. ^{1}H-NMR spectrum of [Ru(*p*-cymene)(ptu)$_2$Cl]SH complex in CD_3OH

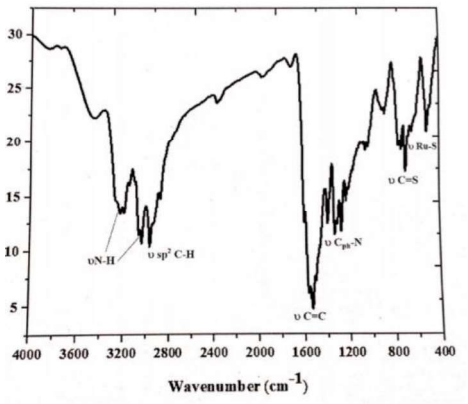

S2. FTIR spectrum of [Ru(*p*-cymene)(ptu)$_2$Cl]SH complex, KBr disk

S 3. Related X-ray data

Table 2. Atomic coordinates (x 10^4) and equivalent isotropic displacement parameters (Å^{2}x 10^3) of [Ru(*p*-cymene)(ptu)$_2$Cl]SH. U(eq) is defined as one third of the trace of the orthogonalized U^{ij} tensor.

	x	y	z	U(eq)
Ru(1)		685(1)	4526(1)	3202(1)
Cl(1)	2188(1)	4246(1)	4421(1)	41(1)
S(1)	4007(1)	3649(1)	2632(1)	35(1)
N(1)	4019(4)	1914(2)	3902(1)	49(1)
C(1)	4784(4)	2282(2)	3164(2)	35(1)
S(2)	2231(1)	6140(1)	2670(1)	38(1)
N(2)	6268(4)	1549(2)	2855(1)	44(1)
C(2)	7319(4)	1702(2)	2081(2)	43(1)
S(3')	7218(2)	-669(1)	4260(1)	104(1)
N(3)	-419(4)	7056(2)	3722(1)	51(1)
C(3)	6291(5)	2209(3)	1405(2)	59(1)
N(4)	1673(4)	8170(2)	2905(2)	58(1)
C(4)	7423(8)	2313(3)	670(2)	83(1)
C(5)	9530(8)	1902(4)	610(3)	98(2)
C(6)	10555(6)	1381(3)	1273(3)	79(1)
C(7)	9454(5)	1282(2)	2008(2)	57(1)
C(8)	1074(4)	7179(2)	3129(2)	40(1)
C(9)	3275(5)	8459(2)	2295(2)	57(1)
C(10)	3160(6)	8486(3)	1523(2)	66(1)
C(11)	4715(8)	8805(3)	951(3)	95(2)
C(12)	6347(9)	9102(4)	1144(5)	123(2)
C(13)	6492(8)	9087(4)	1899(5)	118(2)
C(14)	4954(7)	8765(3)	2489(3)	90(1)
C(15)	-1965(4)	3728(2)	3888(2)	41(1)
C(16)	-989(4)	3182(2)	3306(2)	42(1)
C(17)	-709(4)	3802(2)	2502(2)	37(1)
C(18)	-1422(4)	4973(2)	2264(1)	35(1)
C(19)	-2394(4)	5522(2)	2867(2)	37(1)
C(20)	-2654(4)	4919(2)	3660(2)	40(1)
C(21)	-2237(5)	3093(3)	4742(2)	62(1)
C(22)	-1180(4)	5645(3)	1409(2)	45(1)
C(23)	809(5)	5182(3)	943(2)	70(1)
C(24)	-3107(5)	5727(3)	1007(2)	62(1)

Table 3. Bond lengths [Å] and angles [°] of [Ru(*p*-cymene)(ptu)$_2$Cl]SH.

Ru(1)-C(17)	2.159(2)
Ru(1)-C(19)	2.187(2)
Ru(1)-C(18)	2.198(2)
Ru(1)-C(16)	2.203(2)
Ru(1)-C(20)	2.216(2)
Ru(1)-C(15)	2.253(2)
Ru(1)-S(2)	2.3962(7)
Ru(1)-S(1)	2.4106(6)
Ru(1)-Cl(1)	2.4160(6)
S(1)-C(1)	1.710(3)
N(1)-C(1)	1.317(3)
N(1)-H(1A)	0.8600
N(1)-H(1B)	0.8600
C(1)-N(2)	1.338(3)
S(2)-C(8)	1.700(3)
N(2)-C(2)	1.416(3)
N(2)-H(2)	0.8600
C(2)-C(7)	1.381(4)
C(2)-C(3)	1.381(4)
S(3')-H(3')	0.85(4)
N(3)-C(8)	1.324(4)

Table 3. Bond lengths [Å] and angles [°] of [Ru(*p*-cymene)(ptu)$_2$Cl]SH.

N(3)-H(3A)	0.8600
N(3)-H(3B)	0.8600
C(3)-C(4)	1.383(5)
C(3)-H(3)	0.9300
N(4)-C(8)	1.342(4)
N(4)-C(9)	1.424(4)
N(4)-H(4A)	0.8600
C(4)-C(5)	1.361(6)
C(4)-H(4)	0.9300
C(5)-C(6)	1.364(6)
C(5)-H(5)	0.9300
C(6)-C(7)	1.374(5)
C(6)-H(6)	0.9300
C(7)-H(7)	0.9300
C(9)-C(10)	1.369(5)
C(9)-C(14)	1.384(5)
C(10)-C(11)	1.375(5)
C(10)-H(10)	0.9300
C(11)-C(12)	1.349(7)
C(11)-H(11)	0.9300
C(12)-C(13)	1.349(8)
C(12)-H(12)	0.9300
C(13)-C(14)	1.384(7)
C(13)-H(13)	0.9300
C(14)-H(14)	0.9300
C(15)-C(16)	1.387(4)
C(15)-C(20)	1.419(4)
C(15)-C(21)	1.501(4)
C(16)-C(17)	1.422(4)
C(16)-H(16)	0.9300
C(17)-C(18)	1.398(4)
C(17)-H(17)	0.9300
C(18)-C(19)	1.421(4)
C(18)-C(22)	1.513(4)
C(19)-C(20)	1.397(4)
C(19)-H(19)	0.9300
C(20)-H(20)	0.9300
C(21)-H(21A)	0.9600
C(21)-H(21B)	0.9600
C(21)-H(21C)	0.9600
C(22)-C(23)	1.518(4)
C(22)-C(24)	1.526(4)
C(22)-H(22)	0.9800
C(23)-H(23A)	0.9600
C(23)-H(23B)	0.9600

Table 3. Bond lengths [Å] and angles [°] of [Ru(*p*-cymene)(ptu)$_2$Cl]SH.

C(23)-H(23C)	0.9600
C(24)-H(24A)	0.9600
C(24)-H(24B)	0.9600
C(24)-H(24C)	0.9600
C(17)-Ru(1)-C(19)	67.10(10)
C(17)-Ru(1)-C(18)	37.42(10)
C(19)-Ru(1)-C(18)	37.82(9)
C(17)-Ru(1)-C(16)	38.02(10)
C(19)-Ru(1)-C(16)	78.93(10)
C(18)-Ru(1)-C(16)	68.08(10)
C(17)-Ru(1)-C(20)	79.08(10)
C(19)-Ru(1)-C(20)	37.01(9)
C(18)-Ru(1)-C(20)	67.75(9)
C(16)-Ru(1)-C(20)	66.06(11)
C(17)-Ru(1)-C(15)	67.14(10)
C(19)-Ru(1)-C(15)	66.90(10)
C(18)-Ru(1)-C(15)	80.18(9)
C(16)-Ru(1)-C(15)	36.25(10)
C(20)-Ru(1)-C(15)	37.01(10)
C(17)-Ru(1)-S(2)	124.07(7)
C(19)-Ru(1)-S(2)	91.63(7)
C(18)-Ru(1)-S(2)	95.05(7)
C(16)-Ru(1)-S(2)	161.98(7)
C(20)-Ru(1)-S(2)	114.55(8)
C(15)-Ru(1)-S(2)	150.77(8)
C(17)-Ru(1)-S(1)	86.06(7)
C(19)-Ru(1)-S(1)	140.98(7)
C(18)-Ru(1)-S(1)	104.50(7)
C(16)-Ru(1)-S(1)	97.44(8)
C(20)-Ru(1)-S(1)	163.27(8)
C(15)-Ru(1)-S(1)	129.00(8)
S(2)-Ru(1)-S(1)	80.19(2)
C(17)-Ru(1)-Cl(1)	146.74(7)
C(19)-Ru(1)-Cl(1)	127.58(7)
C(18)-Ru(1)-Cl(1)	165.08(7)
C(16)-Ru(1)-Cl(1)	110.31(7)
C(20)-Ru(1)-Cl(1)	97.78(7)
C(15)-Ru(1)-Cl(1)	90.31(7)
S(2)-Ru(1)-Cl(1)	87.63(2)
S(1)-Ru(1)-Cl(1)	90.42(2)
C(1)-S(1)-Ru(1)	110.81(9)
C(1)-N(1)-H(1A)	120.0
C(1)-N(1)-H(1B)	120.0
H(1A)-N(1)-H(1B)	120.0
N(1)-C(1)-N(2)	117.0(2)

Table 3. Bond lengths [Å] and angles [°] of [Ru(*p*-cymene)(ptu)$_2$Cl]SH.

N(1)-C(1)-S(1)	121.93(19)
N(2)-C(1)-S(1)	121.0(2)
C(8)-S(2)-Ru(1)	110.86(10)
C(1)-N(2)-C(2)	129.1(2)
C(1)-N(2)-H(2)	115.4
C(2)-N(2)-H(2)	115.4
C(7)-C(2)-C(3)	119.2(3)
C(7)-C(2)-N(2)	117.8(3)
C(3)-C(2)-N(2)	122.9(3)
C(8)-N(3)-H(3A)	120.0
C(8)-N(3)-H(3B)	120.0
H(3A)-N(3)-H(3B)	120.0
C(2)-C(3)-C(4)	119.5(3)
C(2)-C(3)-H(3)	120.2
C(4)-C(3)-H(3)	120.2
C(8)-N(4)-C(9)	125.6(2)
C(8)-N(4)-H(4A)	117.2
C(9)-N(4)-H(4A)	117.2
C(5)-C(4)-C(3)	120.4(4)
C(5)-C(4)-H(4)	119.8
C(3)-C(4)-H(4)	119.8
C(4)-C(5)-C(6)	120.6(4)
C(4)-C(5)-H(5)	119.7
C(6)-C(5)-H(5)	119.7
C(5)-C(6)-C(7)	119.6(4)
C(5)-C(6)-H(6)	120.2
C(7)-C(6)-H(6)	120.2
C(6)-C(7)-C(2)	120.6(4)
C(6)-C(7)-H(7)	119.7
C(2)-C(7)-H(7)	119.7
N(3)-C(8)-N(4)	117.0(2)
N(3)-C(8)-S(2)	122.6(2)
N(4)-C(8)-S(2)	120.4(2)
C(10)-C(9)-C(14)	119.5(4)
C(10)-C(9)-N(4)	122.1(3)
C(14)-C(9)-N(4)	118.4(4)
C(9)-C(10)-C(11)	119.8(4)
C(9)-C(10)-H(10)	120.1
C(11)-C(10)-H(10)	120.1
C(12)-C(11)-C(10)	120.4(5)
C(12)-C(11)-H(11)	119.8
C(10)-C(11)-H(11)	119.8
C(13)-C(12)-C(11)	120.9(6)
C(13)-C(12)-H(12)	119.6
C(11)-C(12)-H(12)	119.6

Table 3. Bond lengths [Å] and angles [°] of [Ru(*p*-cymene)(ptu)$_2$Cl]SH.

C(12)-C(13)-C(14)	120.0(5)
C(12)-C(13)-H(13)	120.0
C(14)-C(13)-H(13)	120.0
C(9)-C(14)-C(13)	119.4(5)
C(9)-C(14)-H(14)	120.3
C(13)-C(14)-H(14)	120.3
C(16)-C(15)-C(20)	118.3(2)
C(16)-C(15)-C(21)	121.6(3)
C(20)-C(15)-C(21)	120.1(3)
C(16)-C(15)-Ru(1)	69.91(15)
C(20)-C(15)-Ru(1)	70.05(14)
C(21)-C(15)-Ru(1)	130.22(18)
C(15)-C(16)-C(17)	120.7(3)
C(15)-C(16)-Ru(1)	73.84(15)
C(17)-C(16)-Ru(1)	69.31(14)
C(15)-C(16)-H(16)	119.6
C(17)-C(16)-H(16)	119.6
Ru(1)-C(16)-H(16)	129.7
C(18)-C(17)-C(16)	121.8(2)
C(18)-C(17)-Ru(1)	72.80(14)
C(16)-C(17)-Ru(1)	72.67(15)
C(18)-C(17)-H(17)	119.1
C(16)-C(17)-H(17)	119.1
Ru(1)-C(17)-H(17)	127.6
C(17)-C(18)-C(19)	116.8(2)
C(17)-C(18)-C(22)	122.7(2)
C(19)-C(18)-C(22)	120.5(2)
C(17)-C(18)-Ru(1)	69.78(14)
C(19)-C(18)-Ru(1)	70.65(13)
C(22)-C(18)-Ru(1)	129.99(17)
C(20)-C(19)-C(18)	121.6(2)
C(20)-C(19)-Ru(1)	72.63(14)
C(18)-C(19)-Ru(1)	71.53(14)
C(20)-C(19)-H(19)	119.2
C(18)-C(19)-H(19)	119.2
Ru(1)-C(19)-H(19)	129.1
C(19)-C(20)-C(15)	120.7(2)
C(19)-C(20)-Ru(1)	70.36(14)
C(15)-C(20)-Ru(1)	72.93(14)
C(19)-C(20)-H(20)	119.6
C(15)-C(20)-H(20)	119.6
Ru(1)-C(20)-H(20)	129.5
C(15)-C(21)-H(21A)	109.5
C(15)-C(21)-H(21B)	109.5
H(21A)-C(21)-H(21B)	109.5

Table 3. Bond lengths [Å] and angles [°] of [Ru(*p*-cymene)(ptu)$_2$Cl]SH.

C(15)-C(21)-H(21C)	109.5
H(21A)-C(21)-H(21C)	109.5
H(21B)-C(21)-H(21C)	109.5
C(18)-C(22)-C(23)	113.8(2)
C(18)-C(22)-C(24)	109.3(2)
C(23)-C(22)-C(24)	110.8(3)
C(18)-C(22)-H(22)	107.6
C(23)-C(22)-H(22)	107.6
C(24)-C(22)-H(22)	107.6
C(22)-C(23)-H(23A)	109.5
C(22)-C(23)-H(23B)	109.5
H(23A)-C(23)-H(23B)	109.5

Table 3. Bond lengths [Å] and angles [°] of [Ru(*p*-cymene)(ptu)$_2$Cl]SH.

C(22)-C(23)-H(23C)	109.5
H(23A)-C(23)-H(23C)	109.5
H(23B)-C(23)-H(23C)	109.5
C(22)-C(24)-H(24A)	109.5
C(22)-C(24)-H(24B)	109.5
H(24A)-C(24)-H(24B)	109.5
C(22)-C(24)-H(24C)	109.5
H(24A)-C(24)-H(24C)	109.5
H(24B)-C(24)-H(24C)	109.5

Symmetry transformations used to generate equivalent atoms:

Table 4. Anisotropic displacement parameters (Å^{2}x 10^3) of [Ru(*p*-cymene)(ptu)$_2$Cl]SH. The anisotropic displacement factor exponent takes the form: $-2\pi^2[h^2a^{*2}U^{11} + ... + 2 h k a^* b^* U^{12}]$

	U^{11}	U^{22}	U^{33}	U^{23}	U^{13}	U^{12}
Ru(1)	22(1)	29(1)	31(1)	-9(1)	-2(1)	-3(1)
Cl(1)	35(1)	51(1)	36(1)	-16(1)	-7(1)	-2(1)
S(1)	29(1)	28(1)	42(1)	-7(1)	3(1)	-1(1)
N(1)	59(2)	34(1)	41(1)	-3(1)	2(1)	2(1)
C(1)	33(1)	30(1)	43(1)	-12(1)	-5(1)	-5(1)
S(2)	34(1)	30(1)	52(1)	-16(1)	4(1)	-7(1)
N(2)	52(1)	27(1)	44(1)	-9(1)	-2(1)	5(1)
C(2)	50(2)	26(1)	52(2)	-16(1)	2(1)	-4(1)
S(3')	161(1)	48(1)	56(1)	-1(1)	8(1)	39(1)
N(3)	68(2)	39(1)	42(1)	-17(1)	-5(1)	4(1)
C(3)	68(2)	50(2)	55(2)	-22(2)	-1(2)	1(2)
N(4)	85(2)	30(1)	60(2)	-17(1)	-10(2)	-6(1)
C(4)	118(4)	68(2)	51(2)	-21(2)	4(2)	1(2)
C(5)	129(4)	64(3)	76(3)	-21(2)	47(3)	-7(3)
C(6)	72(2)	51(2)	102(3)	-28(2)	28(2)	-4(2)
C(7)	55(2)	38(2)	75(2)	-24(2)	5(2)	0(1)
C(8)	48(2)	32(1)	38(1)	-10(1)	-14(1)	2(1)
C(9)	63(2)	23(1)	80(2)	-8(1)	-16(2)	-5(1)
C(10)	73(2)	44(2)	76(2)	-10(2)	1(2)	-18(2)
C(11)	114(4)	49(2)	109(4)	-17(2)	31(3)	-24(2)
C(12)	89(4)	48(3)	210(7)	-24(4)	38(4)	-23(2)
C(13)	69(3)	53(3)	236(7)	-33(4)	-24(4)	-22(2)
C(14)	94(3)	41(2)	143(4)	-19(2)	-46(3)	-13(2)
C(15)	25(1)	56(2)	41(1)	-1(1)	-6(1)	-16(1)
C(16)	35(1)	36(1)	55(2)	-2(1)	-11(1)	-16(1)
C(17)	34(1)	41(2)	43(1)	-16(1)	-6(1)	-12(1)
C(18)	29(1)	44(2)	33(1)	-8(1)	-9(1)	-10(1)

Table 4. Anisotropic displacement parameters ($Å^2 x\ 10^3$) of [Ru(*p*-cymene)$(ptu)_2$Cl]SH. The anisotropic displacement factor exponent takes the form: $-2\pi^2[\ h^2a^{*2}U^{11} + ... + 2\ h\ k\ a^*\ b^*\ U^{12}\ ]$

	U^{11}	U^{22}	U^{33}	U^{23}	U^{13}	U^{12}
C(19)	24(1)	40(1)	43(1)	-7(1)	-9(1)	1(1)
C(20)	22(1)	57(2)	38(1)	-14(1)	-2(1)	-3(1)
C(21)	46(2)	85(2)	45(2)	10(2)	-7(1)	-26(2)
C(22)	47(2)	51(2)	35(1)	-5(1)	-7(1)	-12(1)
C(23)	51(2)	106(3)	39(2)	-5(2)	0(1)	-13(2)
C(24)	52(2)	86(2)	37(2)	-5(2)	-14(1)	-2(2)

Table 5. Hydrogen coordinates (x 10^4) and isotropic displacement parameters ($Å^2 x\ 10^3$) of [Ru(*p*-cymene)$(ptu)_2$Cl]SH

	x	y	z	U(eq)
H(1A)	4475	1230	4162	59
H(1B)	3063	2358	4123	59
H(2)	6634	892	3170	53
H(3A)	-958	7598	3944	61
H(3B)	-850	6435	3884	61
H(3)	4849	2478	1445	71
H(4A)	1035	8673	3151	69
H(4)	6741	2665	213	100
H(5)	10277	1979	112	117
H(6)	11992	1093	1227	95
H(7)	10153	929	2461	69
H(10)	2032	8288	1386	79
H(11)	4642	8817	428	114
H(12)	7386	9320	751	147
H(13)	7626	9294	2024	141
H(14)	5047	8754	3010	107
H(16)	-513	2403	3444	50
H(17)	-33	3418	2124	45
H(19)	-2868	6302	2731	45
H(20)	-3285	5303	4042	48
H(21A)	-2942	3612	5053	92
H(21B)	-3055	2544	4794	92
H(21C)	-890	2719	4926	92
H(22)	-1133	6413	1410	54
H(23A)	864	5645	409	105
H(23B)	2003	5183	1187	105
H(23C)	817	4424	940	105
H(24A)	-2958	6153	465	93
H(24B)	-3244	4982	1026	93
H(24C)	-4332	6096	1278	93
H(3')	8350(60)	-440(30)	4150(20)	74

Table 6. Torsion angles [°] of [Ru(*p*-cymene)$(ptu)_2$Cl]SH.

Ru(1)-S(1)-C(1)-N(1)	-20.1(2)
Ru(1)-S(1)-C(1)-N(2)	162.60(19)
N(1)-C(1)-N(2)-C(2)	178.4(3)
S(1)-C(1)-N(2)-C(2)	-4.2(4)
C(1)-N(2)-C(2)-C(7)	137.0(3)
C(1)-N(2)-C(2)-C(3)	-45.7(4)
C(7)-C(2)-C(3)-C(4)	-1.7(5)
N(2)-C(2)-C(3)-C(4)	-179.0(3)
C(2)-C(3)-C(4)-C(5)	1.1(6)
C(3)-C(4)-C(5)-C(6)	0.2(7)
C(4)-C(5)-C(6)-C(7)	-0.9(6)
C(5)-C(6)-C(7)-C(2)	0.3(5)
C(3)-C(2)-C(7)-C(6)	1.0(4)
N(2)-C(2)-C(7)-C(6)	178.5(3)
C(9)-N(4)-C(8)-N(3)	178.6(3)
C(9)-N(4)-C(8)-S(2)	-0.7(4)
Ru(1)-S(2)-C(8)-N(3)	2.5(3)
Ru(1)-S(2)-C(8)-N(4)	-178.27(19)
C(8)-N(4)-C(9)-C(10)	61.2(4)
C(8)-N(4)-C(9)-C(14)	-121.4(3)
C(14)-C(9)-C(10)-C(11)	0.6(5)
N(4)-C(9)-C(10)-C(11)	177.9(3)
C(9)-C(10)-C(11)-C(12)	-0.6(6)
C(10)-C(11)-C(12)-C(13)	0.3(7)
C(11)-C(12)-C(13)-C(14)	0.0(8)
C(10)-C(9)-C(14)-C(13)	-0.3(5)
N(4)-C(9)-C(14)-C(13)	-177.7(3)
C(12)-C(13)-C(14)-C(9)	0.0(7)
C(20)-C(15)-C(16)-C(17)	-0.7(4)
C(21)-C(15)-C(16)-C(17)	-178.7(2)
Ru(1)-C(15)-C(16)-C(17)	-53.1(2)
C(20)-C(15)-C(16)-Ru(1)	52.5(2)

Table 6. Torsion angles [°] of [Ru(*p*-cymene)(ptu)$_2$Cl]SH.

C(21)-C(15)-C(16)-Ru(1)	-125.6(2)
C(15)-C(16)-C(17)-C(18)	-0.9(4)
Ru(1)-C(16)-C(17)-C(18)	-56.1(2)
C(15)-C(16)-C(17)-Ru(1)	55.2(2)
C(16)-C(17)-C(18)-C(19)	1.6(3)
Ru(1)-C(17)-C(18)-C(19)	-54.39(19)
C(16)-C(17)-C(18)-C(22)	-178.7(2)
Ru(1)-C(17)-C(18)-C(22)	125.3(2)
C(16)-C(17)-C(18)-Ru(1)	56.0(2)
C(17)-C(18)-C(19)-C(20)	-0.9(3)
C(22)-C(18)-C(19)-C(20)	179.4(2)
Ru(1)-C(18)-C(19)-C(20)	-54.9(2)
C(17)-C(18)-C(19)-Ru(1)	53.96(19)
C(22)-C(18)-C(19)-Ru(1)	-125.7(2)
C(18)-C(19)-C(20)-C(15)	-0.5(4)

Table 6. Torsion angles [°] of [Ru(*p*-cymene)(ptu)$_2$Cl]SH.

Ru(1)-C(19)-C(20)-C(15)	-54.9(2)
C(18)-C(19)-C(20)-Ru(1)	54.4(2)
C(16)-C(15)-C(20)-C(19)	1.3(4)
C(21)-C(15)-C(20)-C(19)	179.4(2)
Ru(1)-C(15)-C(20)-C(19)	53.7(2)
C(16)-C(15)-C(20)-Ru(1)	-52.4(2)
C(21)-C(15)-C(20)-Ru(1)	125.7(2)
C(17)-C(18)-C(22)-C(23)	-33.9(4)
C(19)-C(18)-C(22)-C(23)	145.7(3)
Ru(1)-C(18)-C(22)-C(23)	56.2(4)
C(17)-C(18)-C(22)-C(24)	90.6(3)
C(19)-C(18)-C(22)-C(24)	-89.8(3)
Ru(1)-C(18)-C(22)-C(24)	-179.3(2)

Symmetry transformations used to generate equivalent atoms:

Table 7. Hydrogen bonds of [Ru(*p*-cymene)(ptu)$_2$Cl]SH [Å and °].

D-H...A	d(D-H)	d(H...A)	d(D...A)	<(DHA)
(1)-H(1A)...S(3')	0.86	2.61	3.374(2)	148.9
N(1)-H(1B)...Cl(1)	0.86	2.50	3.231(2)	143.1
N(2)-H(2)...S(3')	0.86	2.33	3.175(2)	166.2
N(3)-H(3A)...S(3')#1	0.86	2.40	3.240(2)	166.2

Symmetry transformations used to generate equivalent atoms: #1 x-1,y+1,z

Least-squares planes (x,y,z in crystal coordinates) and deviations from them
(* indicates atom used to define plane)
4.7415 (0.0156) x + 7.1502 (0.0058) y - 5.8516 (0.0524) z = 4.7415 (0.0210)
* -1.0014 (0.0035) C3
* 0.1935 (0.0008) N4
* 0.0396 (0.0043) C4
* 0.7803 (0.0039) C5
* 0.5054 (0.0036) C6
* -0.5174 (0.0044) C7
Rms deviation of fitted atoms = 0.6019
- 1.9834 (0.0094) x + 10.5791 (0.0108) y + 0.5997 (0.0292) z = 8.4387 (0.0167)

Angle to previous plane (with approximate esd) = 75.187 (0.105)
* -0.0021 (0.0023) C9
* 0.0029 (0.0025) C10
* -0.0019 (0.0029) C11
* 0.0000 (0.0036) C12
* 0.0008 (0.0035) C13
* 0.0003 (0.0027) C14
Rms deviation of fitted atoms = 0.0017